

Efficient Non-dissociative Activation of Dinitrogen to Ammonia over Li Promoted Ru Nanoparticles at Low Pressure

Jianwei Zheng,^{†[a]} Fenglin Liao,^{†[a]} Simson Wu,^{†[a]} Glenn Jones,^[b] Tian-Yi Chen,^[a] Joshua Fellowes,^[a] Tim Sudmeier,^[a] Ian J. McPherson,^[a] Ian Wilkinson^[c] and Shik Chi Edman Tsang^{*[a]}

Abstract: There is an exciting possibility to decentralize ammonia synthesis for fertilizer production or energy store without carbon emission from H₂ obtained from renewables at small units operated at lower pressure. However, no suitable catalyst is yet developed. Ru catalysts are known to be promoted by heavier alkali dopants. Instead of using higher alkali metals down in periodic table, Li is hereby found to give the highest rate due to surface polarisation despite its poorest electron donating ability. This exceptional promotion rate renders Ru-Li catalysts suitable for the synthesis, which outclasses industrial Fe counterparts by at least 195 folds. Akin to enzyme catalysis, it is for the first time shown that Ru-Li catalysts hydrogenate end-on adsorbed N₂ stabilized by Li⁺ on Ru terrace sites to ammonia in stepwise manner, in contrast to typical N₂ dissociation on stepped sites adopted by Ru-Cs counterparts, giving new insights in activating N₂ by metallic catalysts.

Introduction

Synthetic ammonia has provided fertilizers required for significant increases in food production around the world. The basis for producing ammonia is the Haber-Bosch (HB) process, which was developed in the early 20th century and is without significant change after a century of intensive development.^[1] As one of the greatest known technical innovations, the HB process is currently the second largest industrial scale chemical process. However, around 80% of the HB process uses natural gas as feedstock for the formation and purification of hydrogen associating with fossil-fuel consumption and carbon emissions.^[2] Recently, electric power generated from renewable energy sources such as wind, solar and tidal, at smaller units has become more technically and economically viable, which not only provides for local grid use but can also be used to produce hydrogen via electrolysis of water for green ammonia synthesis under mild conditions. It has been suggested that such an integrated, electrically powered process would facilitate the miniaturization of ammonia synthesis to enable local scale, distributed energy storage (Scheme S1). This new electrolysis Haber-Bosch (eHB) would therefore remove

carbon from the production of ammonia, decreasing emissions associated with fertilizer use while also providing an alternative to hydrogen as a means of energy storage.^[3]

There have been some recent studies to employ lower temperatures in ammonia synthesis. For the miniaturization, the main challenge to the new process is perhaps how to produce ammonia at lower pressure with recycling unreacted substrates (< 5 MPa) without using expensive pressure ramping and cumbersome high pressure installations. Thus, hydrogen manufactured from an electrolyser at low pressure would require coupling with an efficient catalyst to achieve high ammonia production rate in smaller and flexible eHB units for deployment.

In the traditional industrial HB process, ammonia is synthesized via prior dissociation of adsorbed N₂, followed by hydrogenation using H₂. In order to obtain optimal productivity, the reaction conditions are usually set in a temperature regime of 723–773 K and particularly with high pressure range of 15–30 MPa and a maximal flow of reactant gases.^[4] A milder process based on N₂ and H₂ dissociation on catalyst surface would, therefore require the surface does not bind the N and H atoms too strongly while keeping the barrier for N₂ dissociation low. However, the barrier to N₂ dissociative adsorption on a specific catalyst surface is found to be inversely related to the stability of adsorbed N, the so-called scaling relation, leading to the difficulty to identify new HB catalysts to work at more moderate conditions.^[5] By contrast, photochemical, electrochemical and enzymatic routes for ammonia synthesis at mild conditions with non-dissociative activation of N₂ using H⁺ and excited electrons have been explored.^[6] The stepwise hydrogenation of adsorbed N₂ to ammonia without the initial N₂ dissociation might circumvent this scaling relation limitations and offer a new way to promote direct hydrogenation of N₂ to ammonia at low pressure.^[7]

A more efficient catalyst for eHB should therefore have a suitable surface potential for more favorable adsorption and activation of nitrogen preferably like the non-dissociative steps under the kinetic controlled conditions. Compared with the Mittasch's Fe catalysts having similar dopant and modifier compositions, Ru is a better candidate for the eHB process as it is relatively active at low pressure.^[8] Due to the high-energy barrier of dissociation of dinitrogen, alkali metals ions (AM, eg. Cs and K) with strong electron donating abilities are generally employed to improve Ru-based catalysts for ammonia synthesis, this is often attributed to enhanced back donation of electrons from the metal to assist N₂ dissociation under H₂ at elevated temperature.^[9] However, Li is rarely studied in detail because of its anticipated inferior electron donation compared to the other AMs.^[1c,9,10] Here, we report an excellent activity of Ru catalysts promoted by Li at low pressure (0.1 to 5 MPa). The exceptional ammonia production rate of this class of catalysts at milder conditions by larger quantity of Ru terrace sites is attributed to

[a] Dr. J. Zheng, Dr. F. Liao, S. Wu, T. Chen, J. Fellowes, T. Sudmeier, Dr. I. J. McPherson, Prof. S.C.E. Tsang
Wolfson Catalysis Centre, Department of Chemistry University of Oxford, Oxford, OX1 3QR, UK
E-mail: edman.tsang@chem.ox.ac.uk

[b] Dr. G. Jones
Johnson Matthey Technology Centre, Blount's Court, Sonning Common, Reading, RG4 9NH, UK

[c] Dr. I. Wilkinson
Siemens plc, CT NTF, Wharf Road, Oxford OX29 4BP (UK)

Supporting information for this article is given via a link at the end of the document.

RESEARCH ARTICLE

both the Li⁺ blockage of N₂ dissociation sites and more importantly to the polarization and stabilization of non-dissociative partially hydrogenated dinitrogen species by surface Li⁺, which is suitable for the new eHB process at lower pressure.

Results and Discussion

Table 1 shows the comparative catalytic performance of Ru, Fe, and Cr-based catalysts for ammonia synthesis. In general, the use of higher temperature and higher pressure will give higher ammonia production rate but different catalysts may give different optimal activities and stabilities under different conditions. In order to develop a low pressure ammonia production process, suitable catalysts should be compared based on their relative activity at different pressure regimes. The commercial Mittasch's Fe catalyst with multiple promoters composed of Fe₃O₄ or Fe₂O₃, Al₂O₃, K₂O, CaO, MgO and SiO₂ (Fig. S1) is evaluated as a benchmark, which displays a good reaction rate of 95,600 $\mu\text{mol g}_{\text{cat}}^{-1}\text{h}^{-1}$ under an operating pressure of 15 MPa at 732 K (entry 7). However, the reaction rate dramatically drops to 3,600 $\mu\text{mol g}_{\text{cat}}^{-1}\text{h}^{-1}$ when reducing the pressure to 1 MPa (entry 8). This shows that the Fe catalyst which has a lower intrinsic activity than Ru is not a good candidate for the eHB process since it is too sensitive to the reducing pressure. In contrast, Ru with outstretched 4d-orbitals can donate more electron density into the anti-bonding orbital of adsorbed N₂ with higher surface binding, thereby facilitating its dissociation and subsequent operation under a lower pressure. As seen from Table 1, Ru based catalysts display consistently higher activity per gram of catalyst than those based on Fe at the

same temperature. In agreement with literature data^[11], the ammonia production rate per gram of catalyst of Ba-promoted Ru on activated carbon (Ba–Ru/AC) is 1.5 times that of Mittasch's Fe (entries 13, 8). The Ru-Cs based catalyst (entry 10) is one of the most active Ru catalysts currently used in the commercial Kellogg process due to the high electron donating ability of Cs.^[12] In contrast, our results clearly indicate that Ba-Ru-Li catalyst outclasses this reported Ru system at comparable temperature and pressure in our desired ranges. The ammonia production rate is 12.9 times that of Mittasch's Fe and 3.7 times that of Ba-Ru/AC at 1 MPa (entries 2, 3, 8 and 13). The superiority of Ba-Ru-Li catalyst is more apparent if activity is expressed per mole of metal showing the substantially lower Ru metal content required in this class of catalysts. On this basis, its activity is almost 195 times that of Mittasch's Fe at 1 MPa and as far as we are aware, it is much better than all systems reported in the literature. Interestingly, the Ba-Ru-Li catalyst shows a higher rate than the Mittasch's Fe catalysts at 15 MPa but under a significantly reduced pressure of 3 MPa (entries 7 and 1). Even evaluated at 0.1 Mpa (one atmosphere) and at ≤ 373 K the Ba-Ru-Li catalyst also gives a considerable activity (entries 4 and 5, see also Fig.S2). In order to further reduce the metal loading of the working catalyst, a catalyst with 0.5 wt% Ru and 0.76 wt% Li (entry 6) was used, which shows the highest rate in terms of moles of ammonia produced per mole of Ru metal at 1 MPa (127.7 mol NH₃ mol⁻¹ Ru hour⁻¹). We note the combination of Ru-Li is clearly more effective than Ru-Cs irrespective of the support material used (entries 9, 10, 14, 15). This combination seems to display a strong synergetic effect enabling a significantly higher ammonia production rate

Table 1: Comparison of reactivity in the reduction of nitrogen to ammonia over Ru, Fe, Cr-based catalysts, along with others from the literature

Entry	Catalyst	Conditions			Catalytic performance				Ref.
		P (MPa)	T (K)	L (wt%)	$K^{\text{[a]}}$	$K^{\text{[b]}}$	TOF ^[c]	Ea ^[d]	
1	Ba-Ru-Li/AC ^[e]	3	732	4.8	106,120	223.5	1.51	53 \pm 3	This work
2	Ba-Ru-Li/AC	1	732	4.8	46,300	97.5	0.66	-	This work
3	Ba-Ru-Li/AC	1	673	4.8	19,600	41.4	0.28	-	This work
4	Ba-Ru-Li/AC	0.1	732	4.8	4,400	9.3	0.06	-	This work
5	Ba-Ru-Li/AC	0.1	398	4.8	6	0.014	N/A	-	This work
6	Ba-Ru-Li/AC	1	732	0.5	6,300	127.7	1.03	N/A	This work
7	Mittasch's Fe ^[f]	15	732	40.5	95,600	13.2	N/A	N/A	This work
8	Mittasch's Fe	1	732	40.5	3,600	0.5	N/A	N/A	This work
9	Ru-Li/MgO	5	732	5.0	59,400	120.1	N/A	59 \pm 2	This work
10	Ru-Cs/MgO	5	732	5.0	39,600	80.0	N/A	130 \pm 10	This work
11	Ba-Fe /AC	5	732	4.6	3000	36.5	N/A	N/A	This work
12	Ba-Fe-Li/AC	5	732	4.6	2400	29.2	N/A	N/A	This work
13	Ba-Ru/AC	1	673	4.9	5269	10.8	0.08	97 \pm 6	This work
14	Ru-Cs/MgO	1	673	6	12,117	20.4	0.03	120	11
15	Ru-Cs/r-CeO ₂	1	673	4	14,266	36	0.03	108	12
16	Ru/C ₁₂ A ₇ :e ⁻	1	673	4	6,089	15.4	0.22	51	11
17	Ru/C ₁₂ A ₇ :e ⁻	1	673	0.3	3,686	67.7	0.98	40	11
18	Cr-LiH	1	648	56.5	11,200	1.0	N/A	64	1c
19	Ru/Ba-Ca(NH ₂) ₂	0.9	633	10	60,000	59.4	0.41	N/A	13

T, temperature; P, pressure; L, Ru loading; k, reaction rate; Ea, activation energy; Ref., Reference; [a] Activity is expressed as the amount (μmol) of ammonia per gram of catalysts per hour. [b] Activity is expressed as the amount (mol) of ammonia per mole of Ru, Fe or Cr per hour; [c] Turnover of frequency, s⁻¹. [d] Activation energy (Ea in kJ/mol) is obtained at temperature range of 673 K to 773 K. [e] 7.6 wt% Li; ⁺0.76 wt% Li. [f] Commercial Fe catalyst having similar compositions as Mittasch's catalyst. N₂ is at a flow of 26 mL min⁻¹ with 3:1 H₂:N₂. XPS indicates the quenched catalyst contains Li⁺, Ba²⁺ and Ru⁰.

than that of Li promoted 1st row transition metal elements, such as Fe-Li (entries 11 and 12).

Structurally delicate Ru/C₁₂A₇:e⁻ and transition metal-LiH

systems such as Cr-LiH (entries 16-19) and other related systems reported in literature have recently attracted great attention as new efficient NH₃-synthesis catalysts at low temperature.^[1c,11,13]

As stated, the use of lower applied pressure in coupling with electrolyzer in the new eHB process is more important provided that higher activity at higher temperature can be maintained at long lifetime. In fact, the comparison of the turnover frequencies (TOFs) by normalizing the exposed metal surfaces makes Ba-Ru-Li favorable than those other reported catalyst systems at comparable Ru loading disregard the higher temperature used (entries 2 and 19).^[13] The activities of Ba-Ru-Li/AC have also been evaluated as functions of temperature and pressure, which are progressively increased beyond experimental errors (Figs. S3a and S3b). Koros Nowak criterion has been applied to evaluate heat or mass transfer limitations over the kinetic data measurements. The rate measurements were carried out with similar metal dispersions but different Ru loadings (Fig. S3c). The observed TOFs were found to be very similar at the same temperature suggesting that heat and mass transfers did not affect the measurements. The catalyst also shows a good activity and stability for 100 h at 732 K under our laboratory study (Fig. S4). It is interesting to note that Li⁺ promotion greatly attenuates the activation energy (48–59 kJmol⁻¹) compared to the typically reported values of 90–120 kJmol⁻¹ for ammonia production from H₂/N₂ over most reported metal catalysts.^[11,12]

It is well accepted that BaO_x is a structural promoter added to reduce the sintering of Ru and the use of AM promoters (Na⁺, K⁺ and Cs⁺) with Fe or Ru nanoparticles can significantly boost their catalytic activity in converting N₂ and H₂ to ammonia.^[8–10] Particularly, electrons are thought to transfer from the AM to the Ru surface under reducing H₂ conditions and thus promote the donation of electron density from Ru into the π^* anti-bonding orbital of N₂ and facilitating its adsorption. **A volcano relationship is obtained when ammonia production rate is plotted against Li⁺ loading with an optimum value at around 15 wt% (Figure 1a and Fig S11).** According to the difference in electronegativity values, the promotion ranking should follow the order: Cs⁺ > K⁺ > Na⁺ > Li⁺. Figure 1b indeed shows that the order of alkali metal promotion is according to the decreasing order of electronegativity at the same loading except for Li which has the highest electronegativity yet also has the best promotion effect on Ba-Ru/AC for ammonia synthesis at low pressure. Fig. S5a. shows that the exceptional low activation energy (53 ± 3 kJmol⁻¹) of the Li-Ru system is accompanied by an unusual positive order with respect to H₂ partial pressure (+1.02) compared to that of the higher alkali promoted Ru catalysts (90–120 kJmol⁻¹) with typical negative reaction orders for hydrogen at comparable conditions (Figure 1c). It is noted that the negative H₂ reaction orders for Na⁺ (-0.48), K⁺ (-0.55), Cs⁺ (-0.58) as compared to pure Ru without alkali (-0.46) are thought to relate to the competition of dissociative adsorption of N₂ by hydrogen bonding on the stepped sites.^[8] Thus, the positive order dependence of H₂ (less competitive to N₂) on active sites for ammonia production over Li⁺ promoted Ru clearly suggests that the binding of nitrogen species by Li⁺ is significantly stronger compared to hydrogen than other alkali at increasing H₂ pressure at 732 K. The hydrogen order is significantly affected by the reaction temperature, as shown in Fig. S5b, indicating the hydrogen inhibition becomes more severe at a lower temperature.^[13,14] However, the hydrogen order still gives +0.26 at 643 K. This clearly implies an alternative mechanism for

the promotion to the catalyzed reaction, giving a stronger adsorption of N species to enable the application of lower applied pressure. Fig. S6 shows that the X-ray pair distribution function (PDF) profile of Li⁺ doped Ru is comparable to that of Ru nanoparticles, which indicates that Li⁺ does not disrupt the metallic bonding of Ru with no alloy formation or interstitial lattice occupation.^[15] The diffraction patterns from wide-angle XRD (Fig. S7a) and synchrotron XRD (Fig. S7b) also indicate that Li⁺ is likely to partly cover the surface of Ru nanoparticles without any formation of new compounds or structures.

As shown in Figs. 1d, S8, and S9, the Ru nanoparticles in the Ba-Ru/AC and Ba-Ru-Li/AC are homogeneously distributed on the carbon support with an average particle size of 2.1 nm and 2.5 nm, respectively. Analysis of the EXAFS at the Ru K edge was also employed to characterize the coordination environment of Ru at atomic level (Table S1, Fig. S10). In the Ba-Ru/AC sample, typical Ru-Ru scattering paths of 2.67 and 3.77 Å from the hexagonal close packed (*hcp*) lattice are observed, respectively corresponding to the first and second layer. The total coordination number of 7.9 generally matches with the reported particle size of Ru. According to previous DFT calculations, the active site on Ru nanoparticle is likely to be on a step-edge so called 'B5-type' site, which offers an exposed three-fold hollow site in close proximity to a bridging site, and to facilitate the dissociative dinitrogen activation.^[16] The B5 site ensures two nitrogen atoms are not bonded to the same Ru atom, which is energetically and stereospecifically (π^* bond of N₂ to metal d-orbitals) more favorable than the situation at flat terrace metal sites.^[16,17] Jacobsen *et al.* showed that an optimal Ru particle size of 1.8–2.5 nm would contain the maximum number of B5-type sites.^[18] Atomic electron energy loss spectroscopy (EELS) mapping was then used to illuminate the distribution of Li⁺ on selected Ru particles as shown in Figure. 1e. Interestingly, the results reveal that Li⁺ might have selectively covered the higher energy stepped sites as seen by the higher local concentration (green pixels). Carbon monoxide (CO) is commonly used as a chemical marker to differentiate adsorption sites on Ru nanoparticles. As seen from Figure 1f, three peaks at 2021 cm⁻¹, 2012 cm⁻¹, and 1980 cm⁻¹, corresponding to mono-(stepped site), multi-(corner site), and bridge-(terrace site) absorption of CO can be inferred.^[19] Clearly, the introduction of Li⁺ blocks the high indexed unsaturated sites leading to a substantial reduction of the mono and multi-dentate peaks, meaning the effective coverage of stepped sites in agreement with the EELS result. The number of exposed Ru metallic sites was determined by CO chemisorption. The values decrease from 78.1 $\mu\text{mol}\cdot\text{g}^{-1}$ to 10.5 $\mu\text{mol}\cdot\text{g}^{-1}$ with a progressive addition of Li⁺ to Ba-Ru/AC, which indeed suggest the high coverage or decoration of Li⁺ on Ru (Fig. S11). The large decrease in exposed metal surface although offers the selective blockage of the stepped sites (far from 100% selectivity) it can also reduce a substantial quantity of exposed terrace sites.

RESEARCH ARTICLE

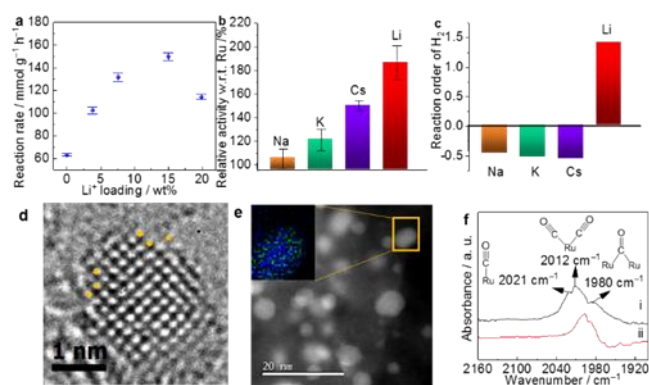


Figure 1. Effect of doping alkali metal ion (AM) on Ba-Ru/AC. **1a.** A volcano relationship between activity and Li^+ loading is obtained indicating that increasingly effective doping before excessive surface coverage. The activities evaluated at 5 MPa, $\text{H}_2/\text{N}_2 = 3$ with H_2 flow of 26 mL/min; 732 K. **1b.** A systematic comparison of AM in promoting Ba-Ru/AC in ammonia synthesis with respect to (w.r.t.) total Ru content; the activities evaluated condition is the same as 1a. **1c.** Reaction order w.r.t. H_2 over AM in promoting Ba-Ru/AC in ammonia synthesis. **1d.** A typical HRTEM image of a selected Ru nanoparticle in Ba-Ru-Li/AC sample. Yellow points represent the stepped atoms in the nanoparticle as B5 sites. **1e.** An atomic EELS mapping (inset) of a STEM image of a Ru nanoparticle (blue), showing Li^+ (green) pre-concentrated in edged/stepped site regions. **1f.** CO chemisorption monitored by ATR-FTIR spectroscopy over i) Ru and ii) Ru-Li nanoparticles. Activity was evaluated for at least 3 times under the same conditions to generate the measurement errors.

DFT calculations have also been carried out to investigate the adsorption energies of alkali metal (AM) onto these surface sites (terrace vs. step sites, see, Figs. S12–14, Tables S2–S4). We employed a $\{10\text{--}15\} 1 \times 2$ surface as a model for the B5 site on a *hcp* Ru crystal. As with the flat surface we explored the stability of different positions for the AM atoms. For high coverage of K^+ and Cs^+ , adsorption of a second adatom (ion) was disfavoured by repulsion from the step to prevent extensive blockage of B5 sites. In contrast, both Li^+ and Na^+ were able to decorate the full length of the step with Li^+ binding significantly more strongly. It appears that the Li^+ preferentially stays at the stepped site presumably due to its small and matching size, filling up the full length of the step edge before moving to the terrace. The DFT calculation results are thus consistent with our experimental results. As the step sites in Ru-Li/AC are covered with Li^+ , the number of B5 sites should be significantly reduced. We believe the selective blockage of the active stepped sites by Li^+ may have forced the ammonia synthesis to adopt an alternative higher energy non-dissociative mechanism on different metal sites (terraces) instead of proceeding via the conventional dissociative pathway on the stepped sites. However, this B5 site poisoning cannot fully explain our observation since one would expect that the partial site poisoning would lower the overall ammonia production rate. Instead, intriguingly, as seen from Figure 2a, the specific activity or turnover frequency (TOF) is significantly improved with an almost 14 fold improvement upon Li^+ addition. Furthermore, as stated, the measured apparent activation energy is dramatically attenuated to 53 kJ mol^{-1} from 97 kJ mol^{-1} (Figure 2b) despite the reduction in number of B5 sites. This indicates that the presence of Li^+ can also somehow greatly promote the non-dissociative reaction steps on terrace sites (Fig. S13).

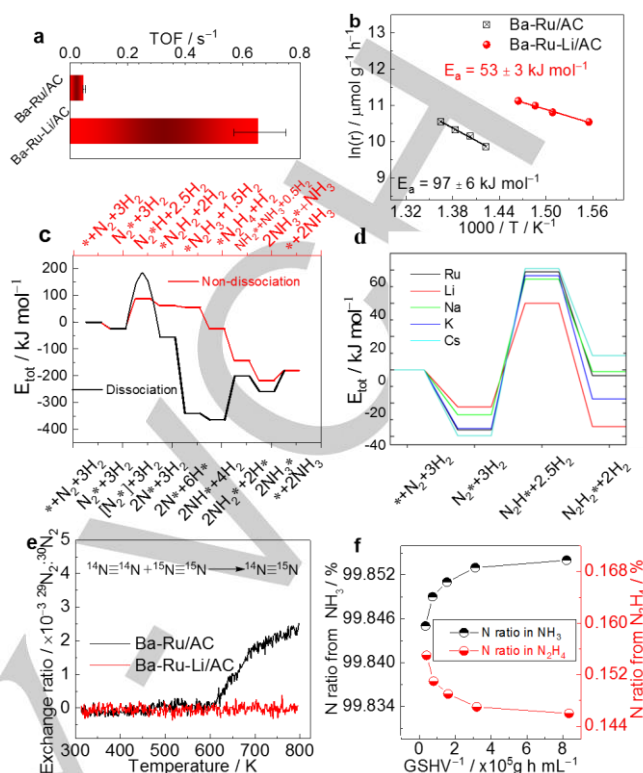


Figure 2. Physicochemical properties and catalytic performance. **2a.** A comparison of turnover frequency (TOF) of Ba-Ru/AC and Ba-Ru-Li/AC samples; the number of exposed Ru atoms was calculated from CO chemisorption assuming $\text{CO}/\text{Ru} = 1$; the activities evaluated at 1 MPa, $\text{H}_2/\text{N}_2 = 3$; 732 K. **2b.** Arrhenius plots of Ba-Ru/AC and Ba-Ru-Li/AC in ammonia synthesis. The reaction condition is at 5 MPa, $\text{H}_2/\text{N}_2 = 3$; 732 K. **2c.** Calculated energy diagrams for ammonia synthesis via dissociative and non-dissociative pathways on Ru-(0001)-(0004) surface; the binding energy, E_{tot} , is defined relative to the energies for the free Ru-(0001)-(0004) surface (*). Structures of the most stable intermediates are shown above and below the energy diagram for dissociative pathway and non-dissociative pathway, respectively; data obtained from Ref. 7. **2d.** Calculations for the most energetic step of adsorbed N_2^* to N_2H^* on Ru(0001) terrace with or without the AM. **2e.** Isotope exchange of $^{28}\text{N}_2$ and $^{30}\text{N}_2$ in 1 atm, flow = 32 mL min^{-1} with a ratio of $^{28}\text{N}_2/^{30}\text{N}_2 = 1:1$; 30, 100 mg catalyst, demonstrating the dissociative mechanism is totally inhibited by Li^+ . **2f.** A residence time study of N selectivity from N_2H_4 ($m/z = 31$) to NH_3 ($m/z = 17$) as a function of GHSV^{-1} , showing N_2H_4 is the intermediate of NH_3 (non-dissociative mechanism), the evaluated condition is similar with 1a.

The reaction energetics of the stepwise non-dissociative pathway on Ru terrace sites have been modelled as compared with that of dissociative pathway on Ru terrace sites by Norskov and co-workers (Figure 2c, Figs. S12, S13).^[7] Despite that there is no convincing experimental proof for this non-dissociative pathway over the metallic Ru terrace surface. As stated by the same authors, the B5 step sites which bind N_2 dissociatively significantly more strongly with a lower energy barrier ($\sim 70 \text{ kJ mol}^{-1}$), and with relatively weaker binding of H_2 than that of terrace sites are the active sites for ammonia synthesis in small nanoparticles.^[7] However, if the step sites are blocked by Li^+ in our case, the calculated first activation energy according to their model for the dissociative pathway is almost twice as high as the stepwise non-dissociative pathway on the terrace sites (see step 3 of Figure 2c in the both processes). Thus, the high energetic

RESEARCH ARTICLE

non-dissociative pathway on the Ru terrace site over lithiated Ru is anticipated to prevail. In order to account for the dramatic rate enhancement in ammonia production upon Li^+ addition, the energy for the formation of the partially hydrogenated di-nitrogen complexes via the non-dissociative pathway on terrace sites over lithiated Ru is greatly reduced in favour of the dissociative barrier from the step sites over the unpromoted Ru nanoparticle. Thus, the calculations for the most energetic uphill step 3 from adsorbed N_2^* to N_2H^* or HN_2^* on Ru(0001) terrace with or without the AM were carried out (Fig. S14) and are shown in Figure 2d and Tables S5-S6. It is interesting to note that the symmetry degeneracy for N_2^* and N_2H^* adsorbed molecules can be altered by the surface Li^+ (polarization) in proximity such that its energy gap is dramatically reduced, presumably due to its exceptional charge density (Figs. S15, S16). Particularly, the N_2H^* has been greatly stabilized when the surface species is placed next to Li^+ , leading to a reduction in energy gap of 0.6 eV at 0 K (or 57.9 kJmol⁻¹).

In order to address whether the non-dissociative pathway on Ru(0001) (0001) terrace sites is more active than that of the dissociative pathway on the stepped sites, we have calculated the kinetic energy barrier of the first hydrogenation of N_2 to form N_2H^* (rate limiting) over the Li^+ modified terrace site compared to the classical dissociative pathway on stepped site.

As seen from Figs. S17-S19 and Table S7, the barrier for non-dissociation pathway over Ru(0001) (0001) terrace site decreases from 112.88 kJmol⁻¹ to 98.41 kJmol⁻¹ with the aid of a small amount of Li^+ on surface (1/8 ML equivalent to one Li^+ in this model). Further increasing the amount of Li^+ (1/4 ML equivalent to two Li^+ in this model) would substantially decrease the barrier to 63.68 kJmol⁻¹ (facilitating H addition to the trans- Li^+ stabilised N_2). Such surface polarization by increasing numbers of Li^+ could even further reduce the overall kinetic barrier for the non-dissociative pathway on terrace sites. In contrast, the barriers for dissociation over the same terrace at the same Li^+ loadings show much higher activation energies (Fig. S18). In comparison, the energy barrier for dissociation of N_2 over Ru-(10-15) stepped site with or without Li^+ (fixed at close proximity) is still around 70 kJmol⁻¹ (see Fig. S19), which is higher than that of the non-dissociative pathway on terrace site. This theoretical model matches with our observation for the dramatic increase in TOF with Li^+ modification on surface (Fig. S11). Thus, both theoretical and experimental data suggest that Li^+ promotes the activity of the non-dissociative pathway on Li^+ modified terrace site more than the classical dissociative pathway on stepped sites.

To illustrate the change in fundamental mechanism from dissociative to non-dissociative pathway, isotopic exchange experiments with $\text{N}^{14}\text{N}^{14}$ and $\text{N}^{15}\text{N}^{15}$ were carried out. Figure 2e shows that onset of chemical exchange of these two dinitrogen molecules begins from 600 K and continues to higher values with further increase temperature over Ba-Ru/AC with presence of a significant number of free stepped sites, as previously observed.^[20] This implies that the predominant mechanism at the stepped sites over this non-lithiated Ru sample is dissociative. Conversely, Ba-Ru-Li/C demonstrates that Li^+ poisoning of these stepped sites totally inhibits the isotopic exchange over the entire temperature range despite the fact that the same catalyst displays

a higher production rate of ammonia when in contact with N_2/H_2 (see Figures. 2a,b). In addition, H_2 dissociation is known to be more favorable than that of dissociative N_2 activation on the remaining terrace sites^[7], hence the ammonia production is not coming from the dissociative pathway but rather from the non-dissociative mechanism on the terrace sites.

The distinction between dissociative and non-dissociative mechanisms lies in the involvement of hydrogenated N-N intermediates prior to N-N bond cleavage. Thus, the product gas over Ba-Ru-Li/AC during ammonia synthesis, trapped in deionized water containing para-(dimethylamino) benzaldehyde at the exit of reactor was monitored, which gave a small detectable peak at around 457 nm in UV-vis spectroscopy indicating N_2H_4 complexation with this compound.^[21] We subsequently analyzed the product gas by online mass spectroscopy at different residence times. As shown in Figure 2f, the residence time of gas composition over the catalyst bed is expressed as inverse of its gas hour space velocity (GHSV⁻¹). The selectivity of N to produce N_2H_4 is significantly increased especially over the Ba-Ru-Li/AC catalyst while NH_3 is decreased at shorter residence time suggesting that N_2H_4 is the primary intermediate of NH_3 . Negligible signal of N_2H_4 was obtained over the non-lithiated Ru sample.

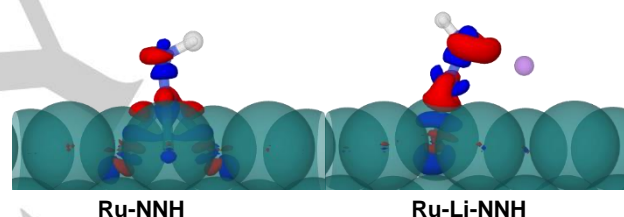


Figure 3. Electron density difference plot. ($p_{\text{total}} - p_{\text{Ru}} - p_{\text{NNH}}$; where p is the electron density of the subscript component); blue negative red positive, which shows the asymmetrical surface polarisation and stabilisation of NNH species by Li^+ (purple ball) to induce electron back donation to π^* region from Ru (see Fig. S16)

Clearly, Li^+ inclusion in Ru catalysts plays a number of key roles in ammonia synthesis. Irrespective of the N_2 activation site, Li^+ with no involvement of p or d orbitals is akin to the recently reported elegant electron promotor of $[\text{Ca}_{24}\text{Al}_{28}\text{O}_{64}](\text{e})_4$ electride which sets free of the electronic donation for Ru promotion from associated downshift of Ru d-band with mixing of p or d-orbitals from the promotor. In this work, Li^+ can also selectively block the N_2 dissociation step site as well as stabilize the partially negatively charged dinitrogen containing intermediates and associated transition states on the terrace sites by the Li^+ . Thus, the electronic promotion and surface stabilization are responsible for the remarkable low pressure ammonia synthesis rate of Ru-Li system (Fig. S2). DFT modelling was also employed to further investigate the degrees of stabilization of adsorbed N_2 and hydrogenated species from the non-dissociative pathway on terrace Ru sites by surface AMs. There is a particularly strong geometric stabilization for Li^+ to stay closer to $\delta\text{-N}_2^*\text{H}$ (the most energetic intermediate, see Figure 2c) than any of the other AMs. It is interesting to note from the calculated electron density difference plots in Figure 3 that the surface Li^+ polarization can clearly break the symmetry of

RESEARCH ARTICLE

N_2H^* and greatly promote the back donation of Ru to N_2H^* (to give δ^- charge) via electrostatic interaction compared to the unpromoted Ru (see Figs S15 and S16). **Further increase in surface Li^+ at close proximity to adsorbed N_2^* gives lower barrier for the non-dissociative pathway on the terrace sites (Table S7).**

As we know that activity of catalyst depends on both the nature of catalytically active sites (activation energy reflects the activity) and their quantitative number of sites per weight of sample used. Li-Ru-Ba/AC showed considerably activity at extremely low temperature regime i.e. 298–373 K and lower pressure than the other state-of-the-art Ru catalysts due to the characteristic nature of catalyst sites created by Li^+ inclusion (blockage of conventionally stepped sites but creating new surface Li^+ polarised terrace Ru sites). The significantly lower activation barrier (see Table 1 and Figure S5) evaluated over this catalyst implies that these new sites can effectively carry out associative mechanism at low temperatures (see the gentle slope at low temperature in Figure S2). However, when reaching the higher temperature regime (say 600 K to 673 K) whereby the dissociative mechanism can then operate over the conventionally state-of-the-art Ru catalysts without Li^+ (stepped sites for dissociative mechanism with higher activation barrier, see Table 1), the numbers of new sites to undergo associative steps in Ba-Ru-Li/AC are limited due to high surface coverage of Li^+ (see chemisorption value) with poor contribution from Li^+ poisoned conventional stepped sites. As a result, in this temperature regime, the activity may not be as good as that of the state-of-the-art Ru catalysts. However, at further increase in temperature to above 732 K, impressive activity can be re-obtained presumably the increase in mobility of Li^+ can set free to the both numbers of sites (see the sharp increase in the slope in Figure S2). We also show that at this high temperature the catalyst is also kinetically stable (Fig. S4).

Conclusion

In short summary, we report a Li-Ru catalyst with a significantly higher NH_3 production rate than previously reported Ru based catalysts in literature at comparably mild temperature and particularly low applied pressure. In the near and medium term, we anticipate that the demand for renewables-based ammonia systems will come primarily from the markets for (i) electrical energy storage, and (ii) anhydrous ammonia fertilizers. At present, the high cost of hydrogen from electrolysis may only allow immediate eHB installation in special locations but a further reduction in electrolyser costs is anticipated. The availability of costly Ru could be an issue to be addressed by further reducing the Ru content from the working catalyst via core-shell or bimetallic approaches. It is noted that Ru is already being used in the industrial Kellogg process though not widely for the ammonia production. In term of mechanism, introduction of Li^+ to block step sites and significantly polarize and stabilize adsorbed dinitrogen intermediates on terrace sites can facilitate non-dissociative over dissociative pathways in favor of the surface N_2 activation relative to H_2 , which may bridge the missing link between enzyme nitrogenase catalyzed N_2 reduction with electrons and protons (non-dissociative) and conventional metal catalysts (dissociative).

We believe this work will inspire researchers to develop further catalytic or electro-catalytic systems for more efficient ammonia production.

Acknowledgments

The support of this project from the IUK-EPSRC of UK (DGE 102000) is gratefully acknowledged. The authors wish to thank the Diamond Light Source, UK for accessing X-rays facilities. GJ also acknowledges the use of the Computing Facilities of Johnson Matthey Technology Centre in the completion of the theoretical part of this work. Further calculations were also conducted on the Center for High Performance Computing (CHPC) in Cape Town South Africa, via their industrial users access. The authors also want to acknowledge Dr Sam French of Johnson Matthey of Billingham, UK for supply and checking their commercial Fe catalyst (KATALCO_{JM}™74-1AR) with our catalyst performance in our reactor.

Keywords: Ammonia synthesis • Lithium • promotion • mechanism • energy storage

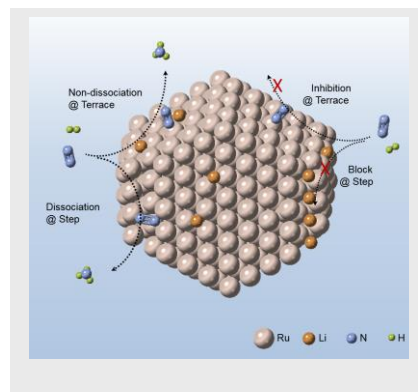
References and notes

- [1] a) J. W. Erisman, M. A. Sutton, J. Galloway, Z. Klimont, W. Winiwarter, *Nat. Geosci.* **2008**, *1*, 636–639; b) P. H. Emmett, S. Brunauer, *J. Am. Chem. Soc.* **1934**, *56*, 35; c) P. K. Wang *et al.*, *Nature Chem.* **2017**, *9*, 64–70.
- [2] E. Worrell, L. Price, M. Neelis, C. Galitsky, Z. Nan, *Tech. Rep.* LBNL-62806 Ernest Orlando Lawrence Berkeley National Laboratory, **2008**.
- [3] a) G. Bolye, Renewable energy: Power for a sustainable future, Oxford University Press: Oxford, U.K., **1997**; b) Y. Lin *et al.*, *Chem.* **2017**, *3*, 712–714.
- [4] A. Mittasch, W. Frankenburg, *Adv. Catal.* **1950**, *2*, 81–104.
- [5] M. M. Rodriguez *et al.*, *Science* **2011**, *334*, 780–783.
- [6] a) T. Oshikiri, K. Ueno, H. Misawa, *Angew. Chem.* **2014**, *126*, 9960–9963; b) J. M. McEnaney *et al.*, *Energy Environ. Sci.* **2017**, *10*, 1621–1630.
- [7] T. H. Rod, A. Logadottir, J. K. Nørskov, *J. Chem. Phys.* **2000**, *112*, 5343–5347.
- [8] C. J. H. Jacobsen, *J. Catal.* **2001**, *200*, 1–3.
- [9] a) K. Aika, H. Hori, A. Ozaki, *J. Catal.* **1972**, *27*, 424–431; b) Y. V. Larichev *et al.*, *J. Phys. Chem. C* **2007**, *111*, 9427–9436.
- [10] G. P. Connor, P. L. Holland, *Catal. Today* **2017**, *286*, 21–40.
- [11] M. Kitano *et al.*, *Nature Chem.* **2012**, *4*, 934–940.
- [12] Z. Ma, *et al.*, *Catal. Sci. Tech.* **2017**, *7*, 191–199.
- [13] M. Kitano *et al.*, *Angew. Chem.* **2018**, *130*, 2678–2682.
- [14] Y. Kadowaki, K. I. Aika, *J. Catal.* **1996**, *161*, 178–185.
- [15] L. J. Santodonato *et al.*, *Nat. Commun.* **2015**, *6*, 5964.
- [16] K. Honkala *et al.*, *Science* **2005**, *307*, 555–558.
- [17] a) S. Dahl *et al.*, *J. Catal.* **2000**, *192*, 391–399; b) S. Dahl *et al.*, *Phys. Rev. Lett.* **1999**, *83*, 1814.
- [18] C. J. H. Jacobsen *et al.*, *J. Mol. Catal. A: Chem.* **2000**, *163*, 19–26.
- [19] a) S. Y. Chin *et al.*, *J. Phys. Chem. B* **2006**, *110*, 871–882; b) A. Kolpin *et al.*, *ACS Catal.* **2017**, *7*, 592–605.
- [20] O. Hinrichsen *et al.*, *J. Catal.* **1997**, *165*, 33–44.
- [21] G. W. Watt, J. D. Chrisp, *Anal. Chem.* **1952**, *24*, 2006–2008.

WILEY-VCH

RESEARCH ARTICLE

Introduction of Li^+ on Ru based catalysts can polarize and stabilize adsorbed dinitrogen on the metal surface, which facilitates the non-dissociative pathway to produce ammonia under mild conditions. Thus, this exceptional promotion renders the Li-Ru catalysts suitable for new green ammonia synthesis at low pressure, which outclasses the commercial Fe counterparts by many folds.



Jianwei Zheng, Fenglin Liao, Simson Wu, Glenn Jones, Tian-Yi Chen, Joshua Fellowes, Tim Sudmeier, Ian J. McPherson, Ian Wilkinson, and Shik Chi Edman Tsang*

Page No. – Page No.

Efficient Non-dissociative Activation of Dinitrogen to Ammonia over Li Promoted Ru Nanoparticles at Low Pressure